

Article

Apparent Quality and Service Performance Evaluation of SCFFC in Tunnel Secondary Lining

Caijin Xie ¹, Tiejun Tao ^{1,*} and Keyu Huang ¹

School of Civil Engineering, Guizhou University, Guiyang 550025, China; xie0803@126.com (C.X.); kyhuang2021@163.com (K.H.)

* Correspondence: tjtao@gzu.edu.cn

Abstract: After removing the mold from the secondary lining concrete of a tunnel, problems such as honeycomb and hemp surface easily occur. To obtain self-compacting fair-faced concrete (SCFFC) that can meet strength requirements and effectively solve the above problems, this research prepared SCFFC with different mix proportions and performed slump expansion, slump, J-ring expansion and mechanical tests. Additionally, this research comprehensively analyzed the SCFFC based on fuzzy mathematics to study its apparent quality and service performance. This research aimed to solve problems such as uneven bubbles and poor bubble diameter in C30 SCFFC, through a combination of defoaming and air entraining by adding defoamer and air-entraining agent according to different proportions for compound treatment. The defoamer dosage was 0.5‰ of that of water reducer, and the air-entraining agent dosage was 0.1‰ of that of cement. The workability and clearance passability of the concrete were optimal. At the same time, the apparent holes in the SCFFC were small, as were their area and quantity. The distribution and apparent color of the SCFFC were uniform. Considering the factors affecting the service performance of concrete and after a comprehensive analysis of the samples' weights, subsection degree, variability, stability, and strength index, this research found that the ratio for obtaining a C30 SCFFC material with the highest apparent quality and service performance was as follows: cement:machine-made sand:crushed dtone:fly-ash:water = 4:8.6:9.3:1:2.2. The water reducer comprised 1.0% of the total mass of the cementitious materials. The defoamer dosage was 0.5‰ of that of water reducer, and the dosage of air-entraining agent was 0.1‰ of that of cement.

Keywords: self-compacting fair-faced concrete (SCFFC); apparent quality; service performance; mechanical test; fuzzy mathematics



Citation: Xie, C.; Tao, T.; Huang, K. Apparent Quality and Service Performance Evaluation of SCFFC in Tunnel Secondary Lining. *Buildings* **2022**, *12*, 479. <https://doi.org/10.3390/buildings12040479>

Academic Editor: Pavel Reiterman

Received: 16 March 2022

Accepted: 11 April 2022

Published: 12 April 2022

Publisher's Note: MDPI stays neutral with regard to jurisdictional claims in published maps and institutional affiliations.



Copyright: © 2022 by the authors. Licensee MDPI, Basel, Switzerland. This article is an open access article distributed under the terms and conditions of the Creative Commons Attribution (CC BY) license (<https://creativecommons.org/licenses/by/4.0/>).

1. Introduction

With the continuous improvement in basic transportation infrastructure around the world, the construction mileage of highways and high-speed railways has increased rapidly. However, traffic routes must traverse many mountains and hills. As a result, bridges and tunnels account for a large proportion of traffic engineering. In the process of tunnel construction, in addition to needing to grasp the mechanical properties of the rock mass of the site, engineers must also consider the supporting structure. The supporting structure of a tunnel is composed of the primary support and secondary lining. Ideally, the primary support bears all the stress transmitted by the surrounding rock, however in reality, after the tunnel excavation, the surrounding rock is deformed and the primary support is squeezed. When the self-supporting capacity of the primary support and surrounding rock reaches its limit, the tunnel's secondary lining begins to bear the load. The secondary lining is the last barrier of the tunnel's supporting structure. At the same time, it is also the most intuitive means for most people to judge whether a tunnel is in a safe or poor state [1–4].

In recent years, tunnel construction engineers, experts and scholars have paid more attention to tunnels' primary supports. However, they have conducted less research on

the service performance and apparent quality of secondary lining materials, especially in the process of tunnel construction in the water-rich karst mountain areas. Typically, when tunnel excavation is completed, the primary support wall is built immediately. However, due to the large amount of water in the rock surrounding the tunnel construction site, the primary support is damaged. Then, a large amount of water seepage occurs in the lining, as shown in Figure 1 [5,6]. At this time, the main treatment measure used on most project sites is to adopt temporary sprayed concrete for plugging and then creating the tunnel's secondary lining. Even if a waterproof layer is set up between the secondary lining and the primary support, moisture will still seep into the secondary lining due to the excessive amount of water. If the secondary lining is composed of an ordinary concrete material, under the action of a large amount of water, the water seeps through the concrete, carries away the relevant chemicals from the concrete, and then precipitates a large number of crystals attached to the lining surface (as shown in Figure 2), which inevitably affect its mechanical properties. During tunnel operation, if water seeps through the secondary lining and falls onto the road surface, it poses a hidden danger [7,8]. In addition, if ordinary concrete is used for the tunnel secondary lining material, after concrete pouring is finished, the surface of the concrete is prone to honeycombing or hemp surface (as shown in Figure 3). In order to improve the apparent quality of the secondary lining, a modified secondary lining trolley must be used to "reprocess" it, as shown in Figure 4 [9]. This process not only prolongs the construction process and is expensive, but most importantly, the secondary lining will have many defects, which will impact its overall stress effect. Therefore, the authors studied the service performance and apparent quality of a tunnel secondary lining concrete material and identified the main factors affecting its service performance and apparent quality, which are of practical significance for tunnel engineering.



Figure 1. Seepage and leakage of tunnel lining.

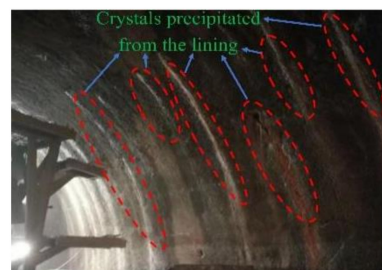


Figure 2. Precipitated crystal of tunnel lining.



Figure 3. Tunnel second lining defect.

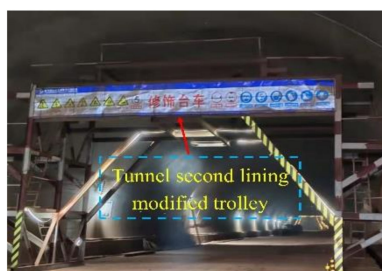


Figure 4. Tunnel second lining modified trolley.

Based on the above purpose, the authors prepared a concrete material that meets service requirements and has high apparent quality—self-compacting fair-faced concrete (SCFFC). SCFFC is a new type of green concrete that combines the advantages of self-compacting concrete (SCC) and fair-faced concrete (FFC). Its advantages are its compactness, ability to pass through gaps, fluidity, less vibration and easy construction. In addition, after removing the mold, the concrete has a smooth surface, few defects and a uniform color. As the filling material of a tunnel's secondary lining, SCFFC can reduce the need for later modification, reduce the need for human and material resources, and reduce the project cost.

Scholars worldwide have conducted considerable research on concrete and achieved successful results. For example: Jayanth et al. added steel fiber to the concrete, and the strength of the concrete increases under the cyclic load, which can effectively restrain the crack width and expansion caused by the concrete failure. They were concerned with the mechanical strength and failure forms of concrete [10]. Wang et al. described the composition and properties of steel-fiber-reinforced concrete in detail and studied the main causes of catastrophes involving the lining after service, but they only focused on the mechanical performance and overall stability of the tunnel lining structure [11]. Abbas and Nehdi were the first to explore the application of mixed-steel-fiber UHPC with different particle sizes in a prefabricated segment of tunnel lining, so that the mechanical properties and component size reductions in tunnel linings were improved [12]. Sangiorgi adopted the experimental design method of the mixture, produced 12 sets of concrete with different mixture ratios, and optimized the mix ratio. He found that adding waste silt to the concrete would not affect the workability of the concrete, and the water absorption of the concrete would be affected by the casting process. However, he only studied the physical and mechanical properties of the concrete and did not study the apparent quality [13]. An et al. studied a shallow-buried rectangular tunnel under vibration load, took fiber-reinforced concrete as a lining structure material, and used finite element software to analyze the seismic performance of the secondary lining structure [14]. Based on the indoor mechanical test results of fiber-reinforced concrete, Belyakov et al. used numerical simulation to study the damage caused to fiber-reinforced concrete used as an underground roadway and as the tunnel lining of a structure under dynamic load [15]. Sheikh and Saif studied the application of steel-fiber-reinforced concrete in the lining of a diversion tunnel. By comparing the use effect of other traditional conventional reinforced concrete linings, they analyzed the construction cost, construction speed, and lining structure stability of steel-fiber-reinforced concrete [16]. Cugat et al. applied fiber-reinforced concrete as a tunnel lining and evaluated the reliability of that lining structure, considering material characteristics and material variability in the actual scale structure [17]. Xu et al. developed the fiber-reinforced coal gangue-based geopolymer concrete (FRCGGPC). They found that the splitting tensile strength of FRCGGPC with steel fiber (SF) and polyester fiber (PF) was higher than that of FRCGGPC with basalt fiber. The fiber combines closely with the coal gangue, which enhances the strength of the matrix material. However, when the amount of fiber is too large, it will reduce the mechanical properties of concrete. The researchers focused on the mechanical properties of concrete, however, they did not study the working and apparent properties of concrete [18]. Based on the thick-walled cylinder

theory, Wang et al. developed a new pressure-resistant concrete material suitable for hydraulic tunnel linings with high water pressure. They conducted tests on the pressure-resistant concrete lining and evaluated its effectiveness [19]. Based on the mechanical response law of concrete under seismic intensity, Xin et al. conducted a series of shaking table tests on ordinary, reinforced and polypropylene-fiber-reinforced concrete as tunnel secondary lining structures to explore whether polypropylene-fiber-reinforced concrete can effectively reduce the seismic response strength and benefit structural stability [20]. Alaloul et al. used fly ash instead of part of cementitious material, rubber powder instead of part of fine aggregate, and silica fume to prepare a new type of SCC. They changed the mix ratio, prepared 13 SCC specimens, and analyzed their mechanical properties [21]. Magbool and Zeyad added five different types of 1% steel fiber and 0.2% hybrid steel fiber (a mixture of all steel fiber types) to concrete to prepare a new SCC. They studied the working and mechanical properties of different types of steel fiber on fresh concrete. At the same time, they found that steel fiber improved the hardening property and toughness index of SCC [22]. Hilal et al. added different proportions of eggshell ash and three kinds of waste plastic fibers to concrete to prepare high-strength self-compacting concrete. They studied the workability and 7-day, 28-day and 90-day compressive and flexural strength of high-strength self-compacting concrete [23]. Kumar et al. replaced 15% cement with fly ash and 15% cement with slag powder to prepare SCC. They added different contents of nano-material-graphene oxide to SCC to improve the strength and toughness of cement-based composites and obtained high strength self-compacting concrete. They aimed to improve the mechanical properties of concrete, however, they did not study the apparent quality of hardened concrete [24]. They all prepare SCC by adding different substitute materials to concrete. Then, its working properties and mechanical properties are studied. Chang et al. simulated the sulfate resistance of FFC and the effect of sulfate on concrete surface quality under sulfate erosion and actual marine environment. They found that sulfate corrodes the surface morphology of FFC. They focused on the changes in the apparent morphology of FFC in a specific environment. They did not delve into the mechanical properties of concrete [25]. In previous studies on tunnel secondary lining concrete materials, scholars have mainly studied the mechanical strength of composite concrete, the influence of vibration load on the secondary lining structure, the damage characteristics of the concrete, and so on. Few researchers have focused on the filling performance and apparent quality of concrete. In particular, research on the combined advantages of SCC and FFC is sparse, and the main factors affecting the service performance and apparent quality of concrete have not been identified.

Therefore, this research took SCFFC as our research object, performed a multiangle analysis, and based on the theory of fuzzy mathematics and through processing the SCFFC test data, quantified each influencing factor to reveal the main factors affecting the service performance and apparent quality of SCFFC. This paper contributes to the research on concrete materials and provides theoretical support and data that can be referenced for the design and construction of secondary tunnel linings.

2. Sample Preparation

This research conducted the test scheme adopted in this study in full accordance with “Technical specification for application of fair-faced concrete” and “Technical specification for application of self-compacting concrete”. The authors obtained the concrete specimens used in the test by mixing cement, machine-made sand, crushed stone, fly ash, admixture and water according to different proportions. First, this research conducted the J-ring and slump tests on the mixed concrete. After determining the relevant parameters, the authors poured concrete into the mold (as shown in Figure 5). Finally, the authors formed the concrete into cube specimens with sides 150 mm long. This research made twelve groups of six specimens, for a total of seventy-two specimens. After analyzing the apparent quality statistics of the concrete specimens, this research conducted uniaxial compression and shear tests. The related experiments in this paper were carried out in the Yanlou PC Factory

of the Guizhou Branch of China Construction Technology Group Co., Ltd. This research determined the optimal proportions for the secondary tunnel lining concrete based on the test results [26–30].

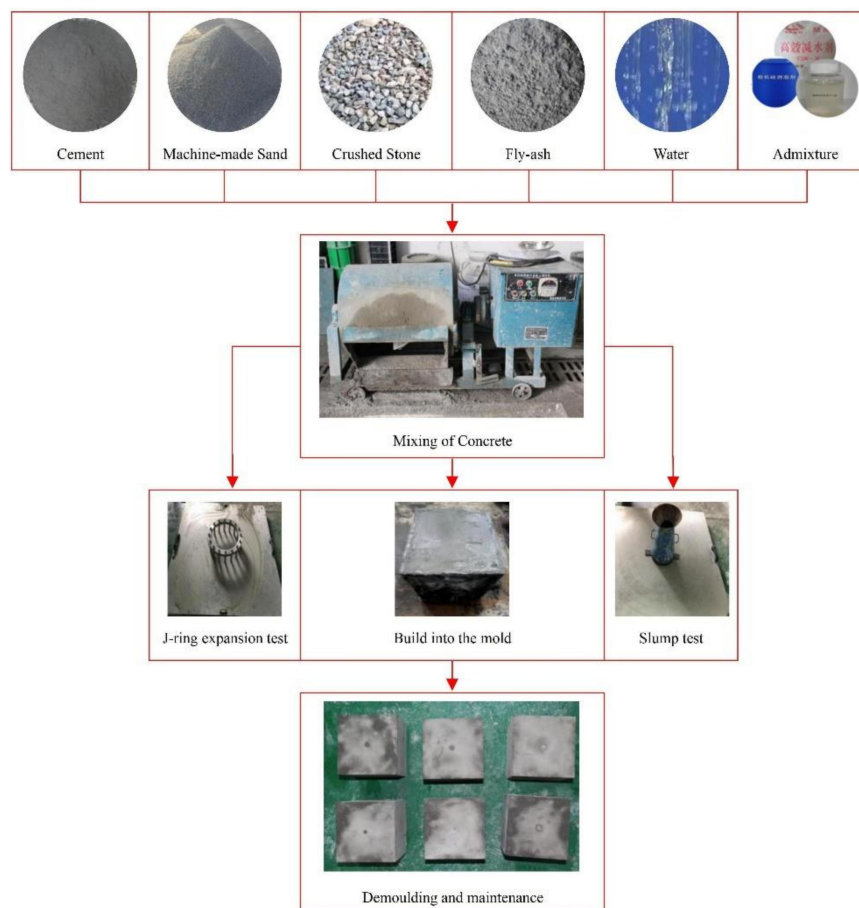


Figure 5. Preparation process of concrete specimen.

3. Factors Controlling Apparent Quality and Service Performance of SCFFC

Our main purpose in this research was to study the apparent quality and service performance of a secondary tunnel lining concrete material. C30 concrete is mostly used in secondary tunnel linings. Therefore, this research used C30 SCFFC for our research. Factory experimenters have rich experience in concrete preparation. Based on their suggestion, this research selected the following SCFFC preparation materials. After a large amount of preparatory work in the early stage of the test, the cement in the raw material of C30 SCFFC was adapted to match Guizhou Linshan PO42.5 cement (its physical and chemical indices are shown in Table 1) to eliminate the color difference on the surface of concrete caused by the addition of mineral admixture to the concrete. The fly ash used was Class F II fly ash produced by Guizhou Huadian Tangzhai Power Generation Co., Ltd. Its performance index is shown in Table 2. The fine aggregate sand used was the same batch of machine-made sand. The fineness modulus was 2.6 and the gradation range was zone II. For the coarse aggregate stone, this research used stones with better grain shape, qualified gradation, and particle sizes within the range 5–20 mm. The admixtures included water reducer, defoamer, and an air-entraining agent. This research used a polycarboxylic acid water reducer, which had little effect on the color of the concrete. Its solid content was 30%, and the water reduction rate was 35%.

Table 1. Guizhou Linshan PO42.5 cement physical and chemical indexes.

Density /g·cm ⁻³	Specific Surface Area /m ² ·kg ⁻¹	Water Requirement of Normal Consistency /%	Setting Time min		Le Chatelier Soundness Test /mm	Mortar Strength /MPa			
			Initial Setting Time/s	Final Setting Time/s		3D Flexural Strength	28D Flexural Strength	3D Compressive Strength	28D Compressive Strength
3.09	340	26.7	229	298	2.0	5.7	7.8	23.6	42.8

Table 2. Fly-ash performance index of Guizhou Huadian Tangzhai Power Generation Co., Ltd.

Fly-Ash Grade	Fineness/%	Ignition Loss/%	Water Content/%	Water Demand Ratio/%
II	23.5	5.2	0.2	84

To improve the apparent quality and service performance of the SCFFC, this research examined the effect of adding defoamer and an air-entraining agent to the concrete. The authors propose the combination of defoaming and air-entraining to solve problems affecting the quality of concrete, such as uneven bubbles and poor bubble diameters. To reduce the bleeding segregation and improve the workability of the concrete in the process of concrete mixing, the authors used a Degusai polyether air-entraining agent to introduce a large number of uniformly distributed, stable, and closed microbubbles into the concrete. Its content was between 0.005% and 0.015% of the weight of the cement. To quickly reduce the surface tension of the material and the surface strength, elasticity, and viscosity of the liquid film, for the defoamer, the authors used organosilicon. Its content was 0.01–0.1% of the weight of the water reducer.

Through the preliminary preparation test, this research obtained the mixture ratio of the C30 SCFFC. The authors conducted J-ring and slump tests on the mixed concrete. Then, this research poured the mixed concrete the molds with side lengths of 150 mm and obtained the test specimens after curing (as shown in Figure 6). Next, the authors analyzed statistics on the quality and apparent defects of each specimen, and finally conducted uniaxial compression and shear test for each specimen. After a statistical analysis of the relevant performance parameters of SCFFC, this research obtained the mixture ratio for C30 SCFFC that can simultaneously guarantee the self-compactness and clear water effect of concrete. Finally, the basic concrete material was adopted in the mix ratio shown in Table 3.

**Figure 6.** Part of the test specimens.

Table 3. Basic material mix ratio of C30 SCFFC.

Number of Groups	Cement /kg·m ⁻³	Machine-Made Sand /kg·m ⁻³	Crushed Stone /kg·m ⁻³	Fly-Ash /kg·m ⁻³	Water /kg·m ⁻³	Water Reducer /%	Water-Binder Ratio	Density /kg·m ⁻³	Defoamer /‰	Air Entraining Agent/‰
Group 1										0.05
Group 2									0.1	0.10
Group 3										0.15
Group 4										0.05
Group 5									0.3	0.10
Group 6	372.94	801.86	867.20	93.23	204.31	1.00	0.44	2800		0.15
Group 7										0.05
Group 8									0.5	0.10
Group 9										0.15
Group 10										0.05
Group 11									0.7	0.10
Group 12										0.15

3.1. Statistics of Slump Expansion, Slump and J-Ring Expansion of SCFFC

The authors mixed the concrete based on Table 3. In order to test the water retention, fluidity, cohesion, and passing quality through gaps in the SCFFC, this research selected test instruments that met industry standards. These included a slump cone, concentric hard square nonabsorbent plate, J-ring, measuring tools, scrapers, etc. First, the slump test was carried out on the SCFFC (see Figure 7). In the first step, the authors wet the concentric hard square nonabsorbent plate and the slump cone, and placed the slump cone in the center of the former, and fixed it. In the second step, the authors filled the slump cone with the mixed and unhardened concrete. In the third step, the authors used a scraper to scrape the concrete to the same plane as the upper edge of the slump cone while cleaning up the surrounding concrete residue. During the whole test process, it did not need to be vibrated. In the fourth step, the authors lifted the slump cone vertically, uniformly and quickly to 300 mm above the original position of the top mouth of the slump cone, taking no more than two seconds. In the fifth step, the authors measured and counted the maximum vertical slump height and lateral maximum expansion of the concrete. Secondly, in the process of concrete expansion, the authors needed to count the time (T_{500}) when the slump expansion reached 500 mm. Finally, the authors carried out the J-ring expansion test on the SCFFC (see Figure 8). In the first step, the authors wet the concentric hard square nonabsorbent plate, slump cone, and J-ring, and placed the J-ring in the center of the concentric hard square nonabsorbent plate. The authors positioned the slump cone upside down and concentric with the J-ring. In the second step, the authors filled inverted slump cone with the mixed and unhardened concrete. In the third step, the authors used a scraper to scrape the concrete to the same plane as the upper edge of the slump cone and simultaneously cleaned up the surrounding concrete residue. During the whole test process, it did not need to be vibrated. In the fourth step, the authors lifted the slump cone vertically, uniformly, and quickly to 300 mm above the original position of the top mouth of the slump cone, taking no more than two seconds. In the fifth step, the authors measured and counted the expansion of the concrete.



(a) Placement of slump cone



(b) Measure and count

Figure 7. SCFFC slump test.



(a) Placement of slump cone and J-ring (b) Measure and count

Figure 8. SCFFC J-ring expansion test.

The SCFFC slump extension, slump and J-ring expansion test results are shown in Figure 9. The statistics of the SCFFC \bar{T}_{500} are shown in Figure 10. According to the requirements of the SCFFC criterion, the slump extension of concrete with first-class filling ability is 550–650 mm, where T_{500} is not less than two seconds. For concrete with first-class passing quality through gaps, the subtractive value of slump expansion and J-ring expansion is in the range 25–50 mm. Through analysis of the test data, this research found that the SCFFC's first-class filling ability was 83.33%, and its first-class rate of passing quality through gaps was 75%. The test results showed that the fluidity, cohesion, and passing quality through gaps of the concrete mix ratio outlined in this paper effectively reached the standards of high-class SCFFC. When the amount of defoamer was constant, with an increase in air-entraining agent, the slump extension and J-ring expansion of the concrete gradually increased, the slump and expansion time fluctuated, and the fluctuation range was small. When the amount of air-entraining agent was constant, with an increase in defoamer, the slump extension, slump, and J-ring expansion of the concrete increased at first and then decreased, and the slump expansion time decreased at first and then increased. Therefore, the defoamer and air-entraining agent must be added and combined according to certain proportions to optimize the workability and passing quality through gaps in the concrete. For this purpose, considering the test data, this research suggests a defoamer dosage of 0.5‰ of that of the water reducer and a dosage of air-entraining agent of 0.1‰ of that of cement.

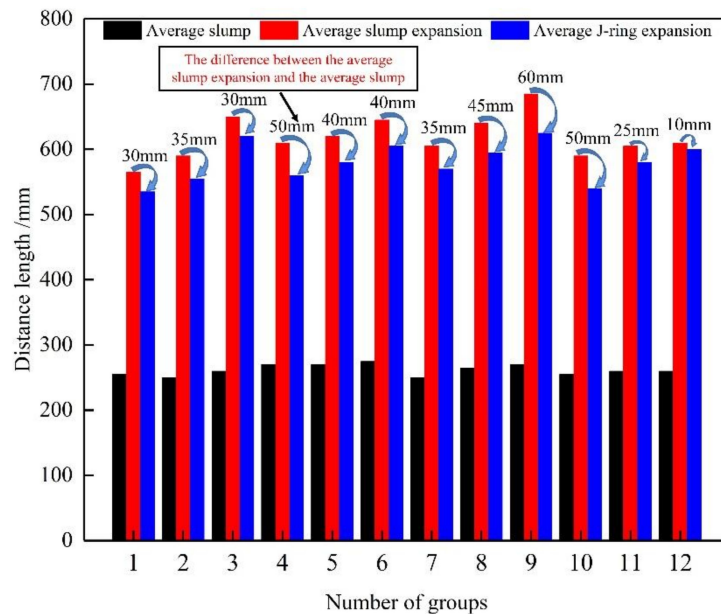


Figure 9. Statistics of apparent quality parameters of SCFFC.

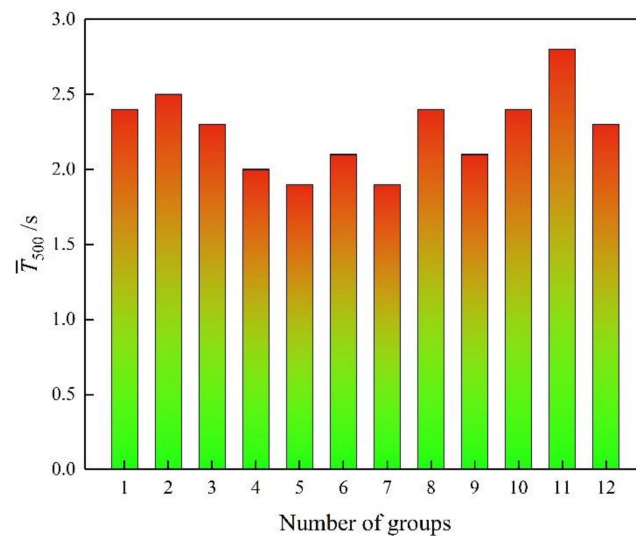


Figure 10. Statistical results of SCFFC \bar{T}_{500} .

3.2. Statistics of Apparent Quality Parameters of SCFFC

For the maintained SCFFC, the authors took pictures of each surface of the specimens. These photos were imported into Image-pro-plus 6.0 software for gray-scale processing, and then the SCFFC's surface holes were statistically analyzed by the software, as shown in Figure 11. The main parameters of SCFFC apparent quality statistics are apparent hole number, apparent hole area, and color uniformity. This research obtained statistical results for the apparent defect density and color uniformity coefficient, as shown in Figure 12. The test results, showed that the effects of adding defoamer and air-entraining agent on the apparent hole number, apparent hole area, and color uniformity of the concrete fluctuated. This phenomenon lacked regularity, and the authors could only find a better proportion from many proportions. When the defoamer dosage was 0.5‰ of that of water reducer and the dosage of air-entraining agent was 0.1‰ of that of cement, the apparent holes in the SCFFC were small, as were their area and quantity. The distribution and apparent color of the SCFFC were uniform. This showed that, with this ratio, the apparent quality of SCFFC was higher, and the occurrences of honeycomb and hemp surface were fewer.

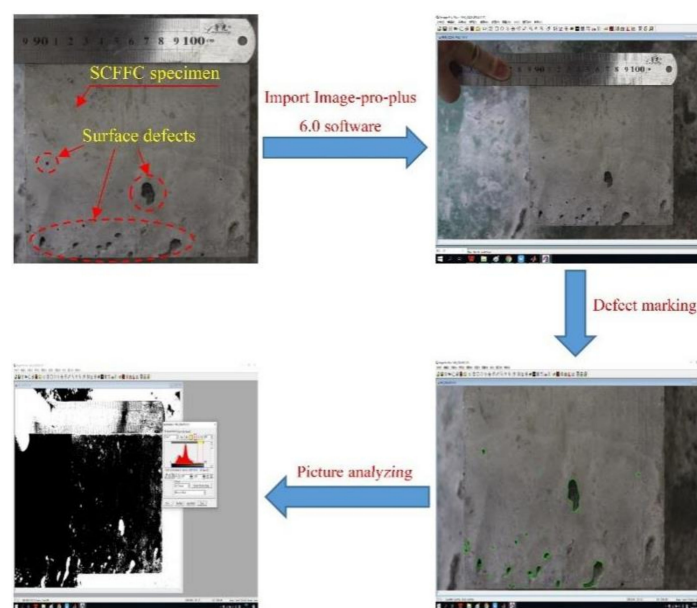


Figure 11. Apparent defect statistics of SCFFC.

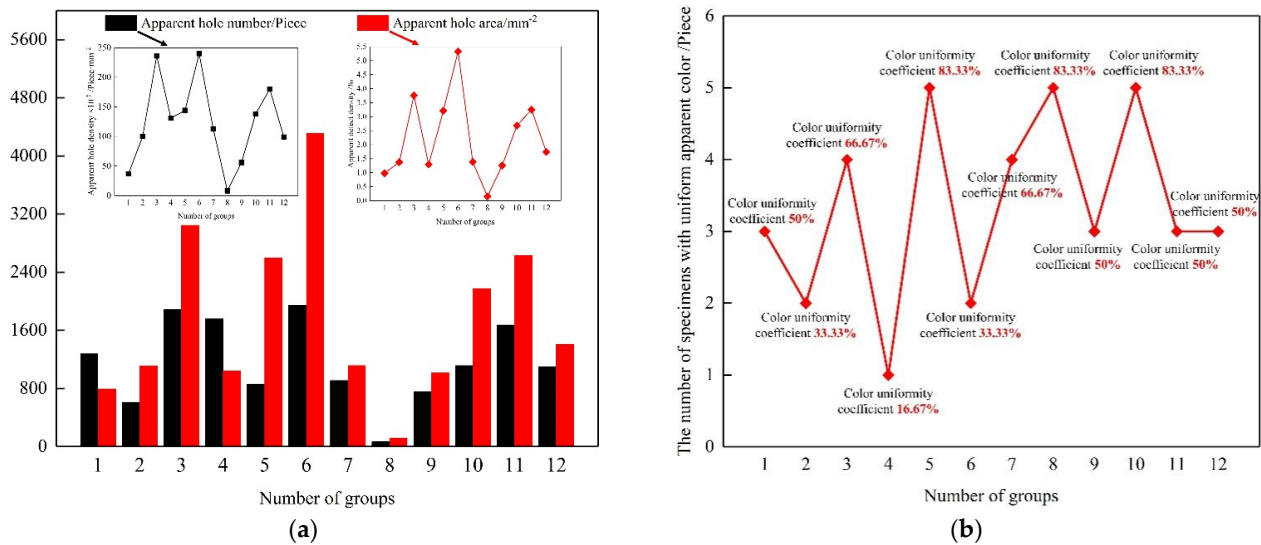


Figure 12. Statistical results of apparent quality parameters of SCFFC. (a) Statistical results of apparent hole number and apparent hole area. (b) The number of specimens with uniform apparent color.

4. Calculation of SCFFC Strength Index

Our purpose in this study was to evaluate the strength of SCFFC under the influence of multiple factors. In this study, the authors took the concrete strength index (*CSI*) as the basis for a comprehensive evaluation of the mechanical properties of concrete. The larger the *CSI*, the stronger the influence on the mechanical properties of the concrete. As the authors still did not know the most important factor affecting the strength of concrete, in the process of evaluating the influencing factors, the authors chose the coefficient of variation method. This method enables the determination of the internal index weights of each constituent element [31–33]. The specific calculation process is as follows:

$$CV_j = \frac{\Delta_j}{\bar{X}_j} (j = 1, 2, \dots, n) \quad (1)$$

In Equation (1), CV_j is the coefficient of variation in the j th index; Δ_j is the standard deviation in the j th index; \bar{X}_j is the average of the j th controlling factor.

$$W_j = \frac{CV_j}{\sum_{j=1}^n CV_j} (j = 1, 2, \dots, n) \quad (2)$$

In Equation (2), W_j is the weight of the j th index.

$$CSI = Q_i \times W_i (j = 1, 2, \dots, n) \quad (3)$$

In Equation (3), Q_i is the membership degree of the j th index.

According to Equations (1)–(3), to determine *CSI*, the authors first need to select the concrete strength index; second, determine each weight index; and the third, establish the membership degree function.

- (1) Selection of the concrete strength index: the uniaxial compressive strength and shear strength of concrete were taken as the evaluation indices of concrete strength, and these two strength values could be obtained by a uniaxial compression test and direct shear test of the concrete.
- (2) Determination of the weight of each index: the authors analyzed the influences of various control factors on the strength indices of the concrete and determined the weight value of each index.

- (3) Establishment of the membership degree function and the calculation of the membership degree: the membership degree function was constructed to establish the mathematical expression between the concrete strength control factors and the strength indices. The ultimate goal was to convert the index values of different dimensions into dimensionless values between zero and one. The higher the degree of membership of a single index, the stronger its impact. The authors used the following formula to calculate the membership degrees of the uniaxial compressive strength and shear strength of the concrete.

$$Q(X) = \begin{cases} 1.0 & X > X_2 \\ 0.1 + 0.9 \frac{X-X_1}{X_2-X_1} & X_1 \leq X \leq X_2 \\ 0.1 & X_1 > X \end{cases} \quad (4)$$

In Equation (4), X_1 is the lower critical value of the concrete strength index and X_2 is the upper critical value of the concrete strength index.

The authors determined the lower and upper critical values of the SCFFC strength index by performing mechanical tests (as shown in Figure 13). The test results are shown in Figure 14. The upper and lower critical values of each strength index are shown in Table 4.

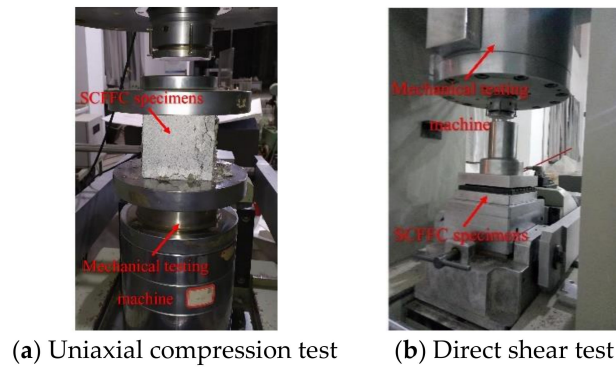


Figure 13. SCFFC mechanical test.

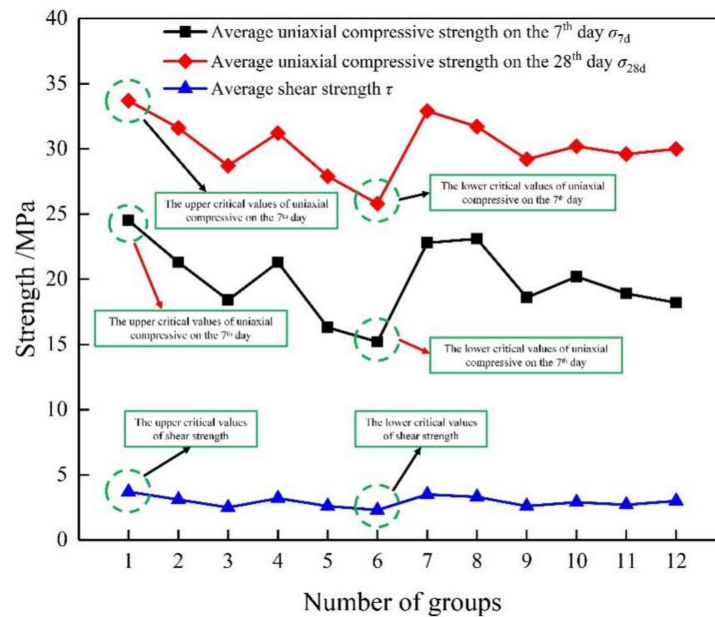


Figure 14. Mechanical strength of SCFFC.

Table 4. The upper and lower critical values of SCFFC strength index.

SCFFC Strength Index	Lower Critical Values X_1 /MPa	Upper Critical Values X_2 /MPa
Uniaxial compressive strength on the 7th day	15.2	24.5
Uniaxial compressive strength on the 28th day	25.8	33.7
Shear strength	2.3	3.7

4.1. Comprehensive Strength Verification and Significance Test of SCFFC

The strength of SCFFC widely fluctuates under the influence of various factors. Therefore, the authors selected three indices, average strength value (\bar{X}), coefficient variation (CV) and stabilization coefficient (SC), to characterize the comprehensive strength of SCFFC. SC was calculated according to the following formula:

$$SC = \begin{cases} \frac{\bar{X}_j - \Delta_\sigma}{\sigma_{MAX}} \\ \frac{\bar{X}_j - \Delta_\tau}{\tau_{MAX}} \end{cases} \quad (5)$$

In Equation (5), Δ_σ is the standard deviation of the SCFFC compressive strength. Δ_τ is the standard deviation of the SCFFC shear strength. σ_{MAX} is the maximum compressive strength of the SCFFC. τ_{MAX} is the maximum shear strength of the SCFFC. Equation (5) illustrates that when Δ_σ and Δ_τ are larger, the CV is larger and the SC is lower.

The authors used SPSS to analyze the variance of the test data and test its significance based on the Duncan method. The results are shown in Table 5, which shows that the additional amounts of defoamer and air-entraining agent, the apparent hole number, and the apparent defect density had substantial effects on the strength of the concrete.

Table 5. Effects of different influencing factors on SCFFC strength.

Influencing Factors		Uniaxial Compressive Strength on the 7th Day/MPa	Uniaxial Compressive Strength on the 28th Day/MPa	Shear Strength/MPa
Defoamer / ‰	0.1	21.4a	31.3a	3.1a
	0.3	17.6c	28.3c	2.7b
	0.5	21.5a	31.3a	3.1a
	0.7	19.1b	29.9b	2.9b
Air entraining agent / ‰	0.05	22.2a	32.0a	3.3a
	0.1	19.9b	30.2b	2.9b
	0.15	17.6c	28.4c	2.6c
Apparent hole density / Piece·mm ⁻²	0–0.001	21.0b	30.8b	3.0b
	0.001–0.0015	19.4c	30.3b	3.0b
	0.0015–0.002	24.5a	33.7a	3.7a
Apparent defect density / ‰	0.002–0.0025	18.5d	28.8c	2.7a
	0–1.5	21.9a	31.7a	3.2a
	1.5–3.0	19.2b	30.1b	3.0b
	3.0–4.5	17.9c	28.7c	2.6c
	4.5–6.0	15.2d	25.8d	2.3d

Explanation: the lowercase letters marked in the table indicate that there is a significant difference at 0.05 level.

4.2. SCFFC Comprehensive Strength Evaluation

The authors substituted the data in Table 5 into Equations (1), (2) and (4). The authors calculated the weight and average membership degree of each index that affected the uniaxial compressive strength and shear strength of the SCFFC, as shown in Tables 6 and 7. The authors also constructed a radar chart based on the data in Tables 6 and 7 (see Figure 15). Our analysis of the radar chart showed that the weight values of the influencing factors of uniaxial compression strength and shear strength were as follows: Apparent defect density > Apparent hole density > Dosage of air entraining agent > Dosage of defoamer.

These results suggest that the apparent defect density of SCFFC was the most important factor affecting its comprehensive strength. However, the average membership degrees of the influencing factors of uniaxial compression strength were as follows: Dosage of defoamer > Dosage of air entraining agent = Apparent defect density > Apparent hole density. These results demonstrate that the apparent hole density was not the main factor affecting the strength of SCFFC. This research comprehensively analyzed the weights and membership degrees of SCFFC compressive strength and shear strength, and preliminarily determined that the apparent defect density was the main factor affecting the strength of SCFFC. To prove this, this research further analyzed the variabilities, stabilities and strength comprehensive indices of the factors influencing SCFFC strength.

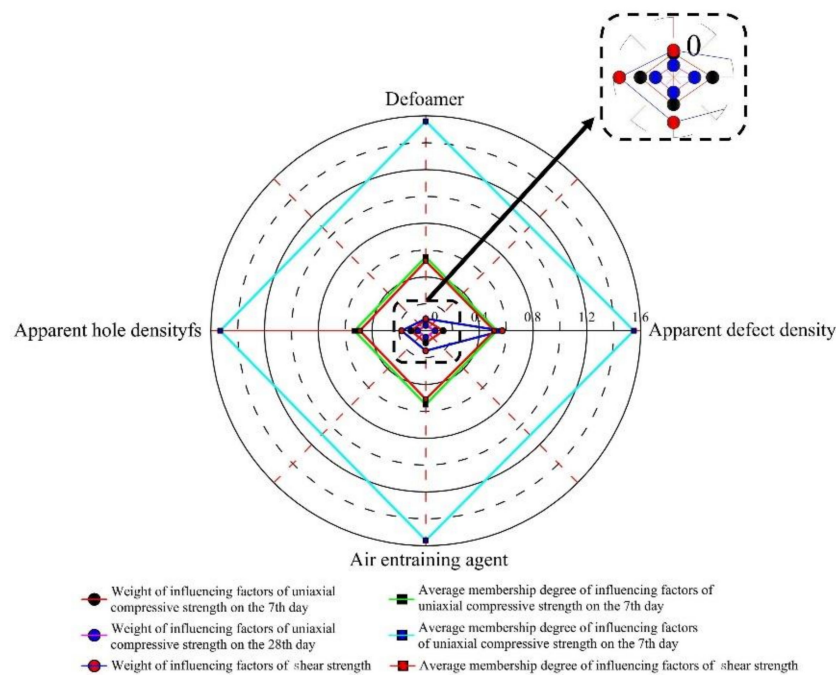


Figure 15. Radar chart of weight and average membership degree of each index of SCFFC strength.

Table 6. Weight and average membership degree of factors affecting uniaxial compressive strength of SCFFC.

Influencing Factors	Uniaxial Compressive Strength									
	7d	28d	7d	28d	7d	28d	7d	28d	7d	28d
	\bar{X}_σ /MPa	Δ_σ /MPa	CV_σ	W_σ	\bar{Q}_σ					
Defoamer	19.9	30.2	1.64	1.24	0.08	0.04	0.08	0.04	0.55	1.56
Air entraining agent	19.9	30.2	1.88	1.47	0.09	0.05	0.09	0.05	0.55	1.56
Apparent hole density	20.9	30.9	2.29	1.78	0.11	0.06	0.11	0.06	0.53	1.53
Apparent defect density	18.6	29.1	2.41	2.17	0.13	0.07	0.13	0.07	0.53	1.55

Table 7. Weight and average membership degree of factors affecting shear strength of SCFFC.

Influencing Factors	Shear Strength				
	\bar{X}_τ /MPa	Δ_τ /MPa	CV_τ	W_τ	\bar{Q}_τ
Defoamer	3.0	0.17	0.06	0.09	0.52
Air entraining agent	2.9	0.29	0.10	0.15	0.51
Apparent hole density	3.1	0.37	0.12	0.18	0.49
Apparent defect density	2.8	1.04	0.37	0.57	0.51

The authors substituted the data obtained in this study into Equations (3) and (5) to obtain, the *SCs* and *CSIs* of the influencing factors (see Table 8). The radar chart in Figure 16 illustrates the *CVs*, *SCs* and *CSIs* of the factors affecting the intensity of SCFFC. The authors comparatively analyzed the factors influencing *CV*, *SC* and *CSI*, and finally determined the most important factor affecting the strength of SCFFC. Tables 9 and 10 show the results of the comparative analysis. After analyzing Tables 9 and 10, this research found the *CV* and *CSI* of the effect of apparent defect density on the uniaxial compressive strength of SCFFC were ranked the largest, and the *SC* was ranked the lowest. The results show that the apparent defect density had the widest variability, the highest stability, and the strongest influence on the comprehensive strength index among the factors influencing the uniaxial compressive strength of SCFFC. The *SC* of the effect of the defoamer addition on the shear strength of SCFFC was ranked the largest, and the *CV* and *CSI* were ranked the lowest. The results show that the defoamer had low variability, high stability and a weak influence on the comprehensive strength index among the factors influencing the shear strength of SCFFC. Although the defoamer had an influence on the shear strength, it cannot be regarded as the most disadvantageous factor. However, the *CV* and *CSI* of the effect of apparent defect density on the shear strength of SCFFC were ranked the largest, and the *SC* was ranked the lowest. The results show that the apparent defect density had the widest variability, the highest stability, and the strongest influence on the comprehensive strength index among the factors influencing the shear strength of SCFFC. Therefore, this research determined that the apparent defect density was the most important factor affecting the strength of SCFFC.

Table 8. *SC* and *CSI* of the influencing factors of SCFFC strength.

Influencing Factors	Uniaxial Compressive Strength				Shear Strength	
	7D		28D		SC	CSI
	SC		CSI			
Defoamer	0.75	0.86	0.04	0.06	0.76	0.05
Air entraining agent	0.74	0.85	0.05	0.08	0.71	0.08
Apparent hole density	0.76	0.86	0.06	0.09	0.74	0.09
Apparent defect density	0.66	0.80	0.07	0.11	0.48	0.29

Our purpose in this study was to solve problems such as honeycomb and hemp surface that occur in the process of filling a secondary tunnel lining with concrete. After our comparative study on the service performance and apparent quality of each concrete material ratio, this research concluded that the C30 SCFFC material with the highest apparent quality and service performance had the following ratio: Cement:Machine-made Sand:Crushed Stone:Fly-ash:Water = 4:8.6:9.3:1:2.2. The water reducer was 1.0% of the total mass of cementitious materials, the defoamer dosage was 0.5% of that of water reducer and the dosage of air-entraining agent was 0.1% of that of cement.

Table 9. Comparison of fuzzy evaluation value of influencing factors of uniaxial compression strength of SCFFC.

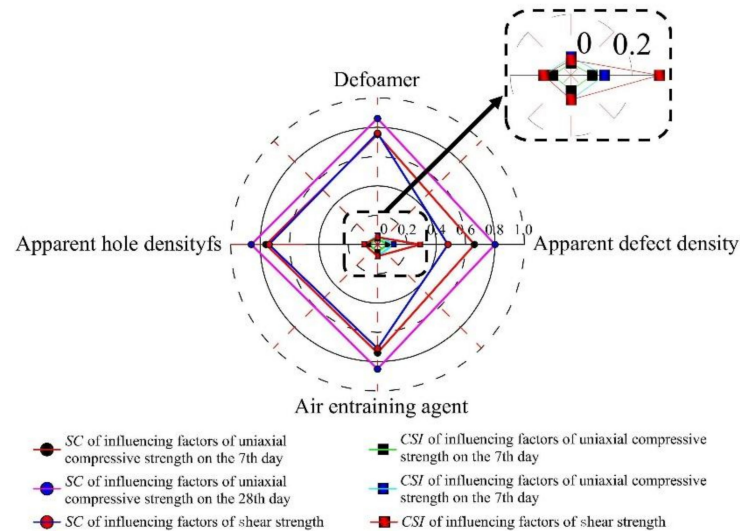
Influencing Factors	Uniaxial Compression Strength											
	CV				SC				CSI			
	7D		28D		7D		28D		7D		28D	
	Result	Rank	Result	Rank	Result	Rank	Result	Rank	Result	Rank	Result	Rank
Defoamer	0.08	4	0.04	4	0.75	2	0.86	1	0.04	4	0.06	4
Air entraining agent	0.09	3	0.05	3	0.74	3	0.85	2	0.05	3	0.08	3
Apparent hole density	0.11	2	0.06	2	0.76	1	0.86	1	0.06	2	0.09	2
Apparent defect density	0.13	1	0.07	1	0.66	4	0.80	3	0.07	1	0.11	1

Explanation: rank from big to small in the table.

Table 10. Comparison of fuzzy evaluation value of influencing factors of shear strength of SCFFC.

Influencing Factors	Shear Strength					
	CV		SC		CSI	
	Result	Rank	Result	Rank	Result	Rank
Defoamer	0.06	4	0.76	1	0.05	4
Air entraining agent	0.10	3	0.71	3	0.08	3
Apparent hole density	0.12	2	0.74	2	0.09	2
Apparent defect density	0.37	1	0.48	4	0.29	1

Explanation: rank from big to small in the table.

**Figure 16.** Radar chart of SC and CSI of each index of SCFFC strength.

5. Conclusions

- (1) The combination of defoaming and air-entraining, by adding the defoamer and air-entraining agent according to different proportions for compound treatment, can solve the problems of uneven bubbles and poor bubble diameter in C30 SCFFC. It can simultaneously ensure that C30 SCFFC has sufficient water retention, fluidity, cohesion, passing quality through gaps, etc. The authors conducted experiments on SCFFC fabricated according to the mix ratio specified in this paper. After analyzing the data on slump expansion, slump, and J-ring expansion, this research concluded that the SCFFC's first-class rate of filling-ability was 83.33%, and its first-class rate of passing quality through gaps was 75%. The test results show that the concrete fabricated according to the mix ratio given in this paper effectively reached the standard of high-class SCFFC.
- (2) When the amount of defoamer was constant, with an increase in air-entraining agent, the slump extension and J-ring expansion of the concrete gradually increased, the slump and expansion time fluctuated, and the fluctuation range was small. When the amount of air-entraining agent was constant, with an increase in defoamer, the slump extension, slump, and J-ring expansion of the concrete increased at first and then decreased, and the slump expansion time decreased at first and then increased. Considering this and the test data, this research concluded that when the defoamer dosage is 0.5‰ of that of the water reducer, and the dosage of air-entraining agent is 0.1‰ of that of cement, the workability and passing quality through gaps of concrete are the highest.
- (3) The effects of the addition of defoamer and air-entraining agent on the apparent hole number, apparent hole area, and color uniformity of the concrete fluctuated. This phenomenon lacked regularity, and this research could only find a better proportion from among many proportions. However, this result also reflected that the additions

of defoamer and air-entraining agent influenced the quality of the concrete, and the additional amounts of both must be strictly controlled. When the defoamer dosage is 0.5‰ of that of the water reducer and the dosage of air-entraining agent is 0.1‰ of that of the cement, the apparent holes in the SCFFC are small, as were their area and quantity. The distribution and apparent color of the SCFFC are uniform.

- (4) This research found that the additional amounts of defoamer and air entraining agent, the apparent hole number and apparent defect density have remarkable effects on the strength of the concrete. Uniaxial compression tests and direct shear tests are conducted on concrete specimens with different mix ratios. This research also performed a comprehensive analysis of the weight, subjection degree, variability, stability, and strength index of the influencing factors based on fuzzy mathematics. This research found that the C30 SCFFC material with the highest apparent quality and service performance has the following ratio: Cement:Machine-made Sand:Crushed Stone:Fly-ash:Water = 4:8.6:9.3:1:2.2. The water reducer is 1.0% of the total mass of the cementitious materials. The defoamer dosage is 0.5‰ of that of the water reducer, and the dosage of the air-entraining agent is 0.1‰ of that of cement. The self-compacting fair-faced concrete prepared according to the above ratio meets the strength requirements and solves problems such as honeycomb and hemp surface in the filling process of secondary tunnel lining concrete.

Author Contributions: Writing—original draft, C.X.; writing—review and editing, T.T.; Data curation, K.H. All authors have read and agreed to the published version of the manuscript.

Funding: The Science and Technology Planning Project of Guizhou Province (Grant Nos. [2020]2Y036).

Institutional Review Board Statement: All participants gave written informed consent in accordance with the Declaration of Helsinki. Ethical approval was not required for this study in accordance with the national and institutional guidelines.

Informed Consent Statement: Informed consent was obtained from all participants involved in the study.

Data Availability Statement: Data is contained within the article.

Acknowledgments: This paper is sponsored by the Science and Technology Planning Project of Guizhou Province (Grant Nos. [2020]2Y036).

Conflicts of Interest: The authors declare no conflict of interest.

References

- Rankoth, C.K.; Hosoda, A.; Iwama, K. Modeling and Verification of Early Age Thermal Stress in Second Lining Concrete of NATM Tunnels. *J. Adv. Concr. Technol.* **2017**, *15*, 213–226. [[CrossRef](#)]
- Wang, R.Y.; Yan, Q.Q.; Tian, B.; Xie, J.D. Effect of Moisture Content and Fiber on the High-Temperature Properties of Tunnel Second Lining Concrete. *J. Highw. Transp. Res. Dev.* **2015**, *9*, 63–68. [[CrossRef](#)]
- Lukic, D.C.; Zlatanovic, E.M.; Jokanovic, I.M. Tunnel lining load with consideration of the rheological properties of rock mass and concrete. *Geomech. Eng.* **2020**, *21*, 53–62. [[CrossRef](#)]
- Lu, C.C.; Hwang, J.H. Damage analysis of the new Sanyi railway tunnel in the 1999 Chi-Chi earthquake: Necessity of second lining reinforcement. *Tunn. Undergr. Space Technol.* **2018**, *73*, 48–59. [[CrossRef](#)]
- Fang, Y.; Guo, J.; Grasmick, J.; Mooney, M. The effect of external water pressure on the liner behavior of large cross-section tunnels. *Tunn. Undergr. Space Technol. Inc. Trenchless Technol. Res.* **2016**, *60*, 80–95. [[CrossRef](#)]
- Zhou, Y.; Su, K.; Wu, H. Hydro-mechanical interaction analysis of high pressure hydraulic tunnel. *Tunn. Undergr. Space Technol. Inc. Trenchless Technol. Res.* **2015**, *47*, 28–34. [[CrossRef](#)]
- Russo, N.; Gastaldi, M.; Marras, P.; Schiavi, L.; Strini, A.; Lollini, F. Effects of load-induced micro-cracks on chloride penetration resistance in different types of concrete. *Mater. Struct.* **2020**, *53*, 143. [[CrossRef](#)]
- Cuenca, E.; Rigamonti, S.; Gastaldo Brac, E.; Ferrara, L. Crystalline Admixture as Healing Promoter in Concrete Exposed to Chloride-Rich Environments: Experimental Study. *J. Mater. Civ. Eng.* **2021**, *33*, 040204911. [[CrossRef](#)]
- Zhang, Y.; Yuan, M.; Liu, C.; Zhang, X.; Yang, B.; Yang, J. Repairing Damaged Tunnel Lining with Small-Size Cavity in Surrounding Rocks. *J. Perform. Constr. Facil.* **2021**, *35*, 06021002. [[CrossRef](#)]
- Jayanth, K.; Prakash, M.N.; Suresh, G.S.; Naveen, B.O. Studies on the behaviour of steel fibre-reinforced concrete under monotonic and repeated cyclic stress in compression. *Arch. Civ. Mech. Eng.* **2022**, *22*, 50. [[CrossRef](#)]

11. Wang, X.; Fan, F.; Lai, J.; Xie, Y. Steel fiber reinforced concrete: A review of its material properties and usage in tunnel lining. *Structures* **2021**, *34*, 1080–1098. [[CrossRef](#)]
12. Abbas, S.; Nehdi, M.L. Mechanical Behavior of Ultrahigh-Performance Concrete Tunnel Lining Segments. *Materials* **2021**, *14*, 2378. [[CrossRef](#)] [[PubMed](#)]
13. Solouki, A.; Tataranni, P.; Sangiorgi, C. Mixture Optimization of Concrete Paving Blocks Containing Waste Silt. *Sustainability* **2022**, *14*, 451. [[CrossRef](#)]
14. An, D.; Chen, Z.; Cui, G. Research on Seismic Performance of Fiber Concrete Lining Structure of Urban Shallow-Buried Rectangular Tunnel in Strong Earthquake Area. *KSCE J. Civ. Eng.* **2021**, *25*, 2378. [[CrossRef](#)]
15. Belyakov, N.; Smirnova, O.; Alekseev, A.; Tan, H. Numerical Simulation of the Mechanical Behavior of Fiber-Reinforced Cement Composites Subjected Dynamic Loading. *Appl. Sci.* **2021**, *11*, 1112. [[CrossRef](#)]
16. Sheikh, K.A.; Saif, A. Steel Fibre-Reinforced Shotcrete as an alternative to conventional concrete tunnel lining: A case study of Gulpur Hydropower Project. *Geomech. Geoengin.* **2020**, *15*, 252–262. [[CrossRef](#)]
17. Cugat, V.; Cavalaro, S.H.P.; Bairán, J.M.; de la Fuente, A. Safety format for the flexural design of tunnel fibre reinforced concrete precast segmental linings. *Tunn. Undergr. Space Technol. Inc. Trenchless Technol. Res.* **2020**, *103*, 103500. [[CrossRef](#)]
18. Xu, Z.; Wu, J.; Zhao, M.; Bai, Z.; Wang, K.; Miao, J.; Tan, Z. Mechanical and microscopic properties of fiber-reinforced coal gangue-based geopolymer concrete. *Nanotechnol. Rev.* **2022**, *11*, 526–543. [[CrossRef](#)]
19. Wang, X.; Liu, L.; Fu, R.; Sun, X. Newly developed pressure adaptable concrete lining for high pressure hydraulic tunnels. *Tunn. Undergr. Space Technol. Inc. Trenchless Technol. Res.* **2020**, *105*, 103570. [[CrossRef](#)]
20. Xin, C.L.; Wang, Z.Z.; Zhou, J.M.; Gao, B. Shaking table tests on seismic behavior of polypropylene fiber reinforced concrete tunnel lining. *Tunn. Undergr. Space Technol. Inc. Trenchless Technol. Res.* **2019**, *88*, 1–15. [[CrossRef](#)]
21. Alaloul, W.S.; Musarat, M.A.; Haruna, S.; Law, K.; Tayeh, B.A.; Rafiq, W.; Ayub, S. Mechanical Properties of Silica Fume Modified High-Volume Fly Ash Rubberized Self-Compacting Concrete. *Sustainability* **2021**, *13*, 5571. [[CrossRef](#)]
22. Magbool, H.M.; Zeyad, A.M. The effect of varied types of steel fibers on the performance of self-compacting concrete modified with volcanic pumice powder. *Mater. Sci.-Pol.* **2021**, *39*, 172–187. [[CrossRef](#)]
23. Hilal, N.; Al Saffar, D.M.; Ali, T.K.M. Effect of egg shell ash and strap plastic waste on properties of high strength sustainable self-compacting concrete. *Arab. J. Geosci.* **2021**, *14*, 291. [[CrossRef](#)]
24. Kumar, B.N.; Abhilash, B.; Naveen Kumar, C.H.; Pavan, S. Effect of Nano Materials on Performance Characteristics of High Strength Self Compacting Concrete. *Assian Res. Assoc.* **2021**, *2*, 26–35. [[CrossRef](#)]
25. Honglei, C.; Zuquan, J.; Penggang, W.; Jianhong, W.; Jian, L. Comprehensive resistance of fair-faced concrete suffering from sulfate attack under marine environments. *Constr. Build. Mater.* **2021**, *277*, 122312. [[CrossRef](#)]
26. Zhang, H.; Zhang, J.; Yang, Y.; Hu, Q.; He, Y.; Wei, P. Effects of asphalt emulsion on the durability of self-compacting concrete. *Constr. Build. Mater.* **2021**, *292*, 123322. [[CrossRef](#)]
27. Grinys, A.; Balamurugan, M.; Augonis, A.; Ivanauskas, E. Mechanical Properties and Durability of Rubberized and Glass Powder Modified Rubberized Concrete for Whitetopping Structures. *Materials* **2021**, *14*, 2321. [[CrossRef](#)]
28. Gnanaraj, S.C.; Chokkalingam, R.B.; Thankam, G.L.; Pothinathan, S.K.M. Influence of Steatite and Fly Ash on the Fresh-Hardened Properties and Micromorphology of Self-Compacting Concrete. *Adv. Mater. Sci. Eng.* **2021**, *2021*, 6627450. [[CrossRef](#)]
29. Belebchouche, C.; Moussaceb, K.; Bensebti, S.E.; Ait-Mokhtar, A.; Hammoudi, A.; Czarnecki, S. Mechanical and Microstructural Properties of Ordinary Concrete with High Additions of Crushed Glass. *Materials* **2021**, *14*, 1872. [[CrossRef](#)]
30. Khoshkbijari, R.K.; Samimi, M.F.; Mohammadi, F.; Talebitaher, P. Effects of Mica and Feldspar as partial cement replacement on the rheological, mechanical and thermal durability of self-compacting mortars. *Constr. Build. Mater.* **2020**, *263*, 120149. [[CrossRef](#)]
31. Yang, X.C.; Ye, H.C.; Li, D.M.; Yu, X.C.; Liu, K.L.; Hu, Q.P.; Hu, Z.H.; Gu, Z.H.; Hu, H.W.; Zhou, L.J.; et al. Assessment of red soil upland fertility in long-term fertilization based on fuzzy mathematics and principal component analysis. *Soil Fertil. Sci. China* **2018**, *3*, 79–84. (In China) [[CrossRef](#)]
32. Terenchuk, S.; Yeremenko, B.; Kartavykh, S.; Nasikovskiy, O. Application of fuzzy mathematics methods to processing geometric parameters of degradation of building structures. *EUREKA Phys. Eng.* **2018**, *1*, 56–62. [[CrossRef](#)]
33. Kuzyakov, O.N.; Kolosova, A.L.; Andreeva, M.A. System for corrosion monitoring in pipeline applying fuzzy logic mathematics. *J. Phys. Conf. Ser.* **2018**, *1015*, 052017. [[CrossRef](#)]